

Electromagnetically driven westward drift and inner-core superrotation in Earth's core

Philip W. Livermore^{a,1}, Rainer Hollerbach^{b,c}, and Andrew Jackson^c

Schools of ^aEarth and Environment and ^bMathematics, University of Leeds, Leeds, West Yorkshire LS2 9JT, United Kingdom; and ^cInstitute for Geophysics, Swiss Federal Institute of Technology, 8092 Zurich, Switzerland

Edited by Gerald Schubert, Institute of Geophysics and Planetary Physics, Los Angeles, CA, and approved August 26, 2013 (received for review April 29, 2013)

A 3D numerical model of the earth's core with a viscosity two orders of magnitude lower than the state of the art suggests a link between the observed westward drift of the magnetic field and superrotation of the inner core. In our model, the axial electromagnetic torque has a dominant influence only at the surface and in the deepest reaches of the core, where it respectively drives a broad westward flow rising to an axisymmetric equatorial jet and imparts an eastward-directed torque on the solid inner core. Subtle changes in the structure of the internal magnetic field may alter not just the magnitude but the direction of these torques. This not only suggests that the quasi-oscillatory nature of inner-core superrotation [Tkalcic H, Young M, Bodin T, Ngo S, Sambridge M (2013) The shuffling rotation of the earth's inner core revealed by earthquake doublets. *Nat Geosci* 6:497–502.] may be driven by decadal changes in the magnetic field, but further that historical periods in which the field exhibited eastward drift were contemporaneous with a westward inner-core rotation. The model further indicates a strong internal shear layer on the tangent cylinder that may be a source of torsional waves inside the core.

geomagnetism | geodynamo

The slow westward drift of the geomagnetic field is one of the best- and longest-known features of the historical field, for which the most likely explanation is a latitudinally dependent westward flow in the outermost outer core (1, 2). Another westward-propagating and possibly related feature is equatorial waves (3), perhaps caused either by advection or instabilities on an equatorial westward jet. However, longer time series provide evidence of periods of eastward drift of the field over the past 3,000 y (4, 5). Although some geodynamo models have reproduced westward drift (6, 7), many rely on thermal winds whose structure is tied to the boundary conditions imposed by the lowermost mantle, which changes only on a timescale of 10–100 million years. A seemingly unrelated phenomenon is the superrotation (relative to the mantle) of the inner core, whose estimates vary from zero to several degrees per year (8). Links between core–surface flows and inner-core rotation are difficult to quantify because a coupling mechanism extending across the entire outer core has remained elusive. There is some evidence of such a coupling through thermal winds in polar regions (9); however, because their amplitude is linked to the mass and thermal flux at the inner-core boundary, unless the inner core is very young, the effect likely is small (10).

The fluid outer core, bounded by the solid inner core and overlying mantle, likely is in a quasi-magnetostrophic balance, in which the forces of pressure, buoyancy, Coriolis, and Lorentz are almost in equilibrium (6). Two key nondimensional parameters in any model are the Ekman and Rossby numbers, measures of viscosity and inertia, respectively, believed to be $\sim 10^{-15}$ and $\sim 10^{-6}$ in the core. However, because of the vast range of temporal and spatial scales in the rapidly rotating system, current models of the geodynamo struggle to reach values of these parameters lower than $E = 10^{-7}$ and $R_o = 10^{-3}$ (6, 7, 11–13). Although scaling laws may attempt an extrapolation to the extreme Earth-like parameters (14), this is difficult over so many orders of magnitude. In

the idealized regime of zero inertia and viscosity, the internal magnetic field \mathbf{B} must satisfy Taylor's constraint (15), in which the axial electromagnetic (EM) torque, \mathcal{T} ,*

$$\mathcal{T}(s) = \int_{C(s)} s([\nabla \times \mathbf{B}] \times \mathbf{B})_{\phi} s \, d\phi \, dz,$$

must integrate to zero over any concentric axially aligned cylinder $C(s)$, where (s, ϕ, z) are cylindrical polar coordinates and $(\)_{\phi}$ denotes the azimuthal component. A full understanding of the earth's core likely is possible only by investigating the dynamics in the vicinity of this limit.

In this study we use a method (*Methods*) that accesses a regime very close to a magnetostrophic balance by seeking steady, inertia-free, ultra-low-viscosity solutions of the geodynamo equations with a prescribed poloidal magnetic field (16) that matches the xCHAOS model (17) to degree 4 at the core–mantle boundary. This technique suppresses the short timescales that prevent current modeling strategies from reaching low viscosities, and we can compute models in the range $E \geq 3 \times 10^{-9}$, two orders of magnitude lower than any previous calculation. By slowly decreasing E in small discrete steps, we could identify well-defined limiting behavior at small E . In numerical models at larger Ekman numbers (18), it is acknowledged that inertia, particularly in a turbulent regime, may play an important role in balancing EM torques. Our model excludes this possibility on the grounds that the Rossby number for the earth is small,[†] and we achieve an “Ekman-state” balance in which viscosity must absorb any

Significance

Seismic probing of the earth's deep interior has shown that the inner core, the solid core of our planet, rotates slightly faster (i.e., eastward) than the rest of the earth. Quite independently, observations of the geomagnetic field provide evidence of westward-drifting features at the edge of the liquid outer core. This paper describes a computer model that suggests that the geomagnetic field itself may provide a link between them: The associated electromagnetic torque currently is westward in the outermost outer core, whereas an equal and opposite torque is applied to the inner core. Decadal changes in the geomagnetic field may cause fluctuations in both these effects, consistent with recent observations of a quasi-oscillatory inner-core rotation rate.

Author contributions: P.W.L., R.H., and A.J. designed research; P.W.L. and R.H. performed research; P.W.L. analyzed data; and P.W.L. wrote the paper.

The authors declare no conflict of interest.

This article is a PNAS Direct Submission.

Freely available online through the PNAS open access option.

¹To whom correspondence should be addressed. E-mail: p.w.livermore@leeds.ac.uk.

*Note that the symbol $\mathcal{T}(s)$ is not to be confused with the Taylor integral, a closely related quantity that differs by a factor of s from the axial EM torque we consider here.

[†]Because viscosity enters into boundary-layer scalings as $E^{1/2}$ rather than E , and further that $E^{1/2} \approx R_o$, arguably both viscosity and inertia may be equally important in the earth's core. However, our goal was to explore the magnetostrophic limit, and as such, we chose to focus attention on the Ekman-state balance at very small viscosity.

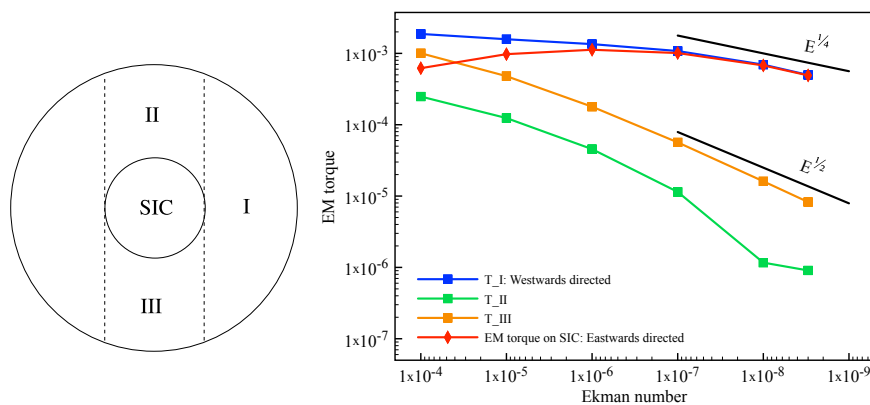


Fig. 1. The absolute value of the net EM torques— T_I , T_{II} , and T_{III} —on each of the three regions I, II, and III and the SIC. The torque on the FOC is dominated by the westward-directed torque in region I, scaling as $E^{1/4}$; the torque on the inner core scales identically and is oppositely oriented. The black lines indicate apparent asymptotic scalings.

unbalanced torque and, indeed, may itself play an important role in the determination of the geostrophic flow (19, 20).

The total axial EM torque integrated over the core may be subdivided into four parts: the three contributions from each of the fluid regions, labeled I, II, and III in Fig. 1, which partition the fluid outer core (FOC), and the torque over the solid inner core (SIC). Surrounded by an electrically insulating mantle, in a steady state this net torque must sum to zero (15); therefore, the axial EM torque on the inner core may be expressed as

$$\int_{SIC} s([\nabla \times \mathbf{B}] \times \mathbf{B})_{\phi} dV = T_{SIC} = -(T_I + T_{II} + T_{III}).$$

Fig. 1 shows how the magnetic field approaches the Taylor limit of $E=0$ in terms of the regionally integrated EM torques. The torques do not scale uniformly as a function of E : that in the outermost outer core (region I) is consistent with a scaling of $E^{1/4}$, dominating the contributions from regions II and III within the tangent cylinder that are bounded by $E^{1/2}$. These different scalings may arise as a result of the increased influence of the boundary conditions on cylinders of largest cylindrical radii, which impart constraints on the magnetic field, not just at either end of the cylinder but everywhere on its surface. Because the westward-directed torque in region I dominates the contributions to the FOC, the SIC experiences an eastward-directed EM torque that scales also as $E^{1/4}$. In our model, the inner core is assumed to be gravitationally locked (21) to the mantle and so cannot move. However, if this constraint is relaxed (22), the

dynamical response of the inner core would be a tendency for an (eastward) superrotation: In this sense, our model is simply an end-member case of a spectrum of models in which the locking gets progressively stronger.

An important quantity in the weak-viscosity limit is the geostrophic flow, $u_g(s)\hat{\phi}$, the azimuthal component of flow averaged on a cylinder $C(s)$. In the absence of inertia but in the presence of weak viscosity, u_g is linked to how quickly T decreases with E , in region I by the relation (6)

$$u_g(s) = \frac{E^{-1/2}(1-s^2)^{1/4}}{4\pi s^2} T(s). \quad [1]$$

Fig. 2A shows the magnitude of the flow decomposed into its geostrophic and ageostrophic components as a function of E . The toroidal-dominated ageostrophic part is almost independent of E , whereas the geostrophic flow (both rms and maximum value) scales as $E^{-1/4}$, as anticipated from Eq. 1 and the scaling $T \sim E^{1/4}$ in region I. For values of E greater than 10^{-7} , the geostrophic flow is a subdominant feature of the model. However, as E is decreased below the threshold at approximately 6×10^{-8} , the geostrophic flow becomes dominant (in rms). Using the scaling of u_g , extrapolating to the earth's core gives dimensional flow velocities of $O(10^{-4})$ m/s, consistent with values derived from studies of core flow (3, 23). Following the derived scalings, the geostrophic flow would dominate the ageostrophic component by a factor of about 100 at $E = 10^{-15}$. However, thermal wind effects that are not included in our model may drive a much stronger ageostrophic flow with an amplitude consistent with typical

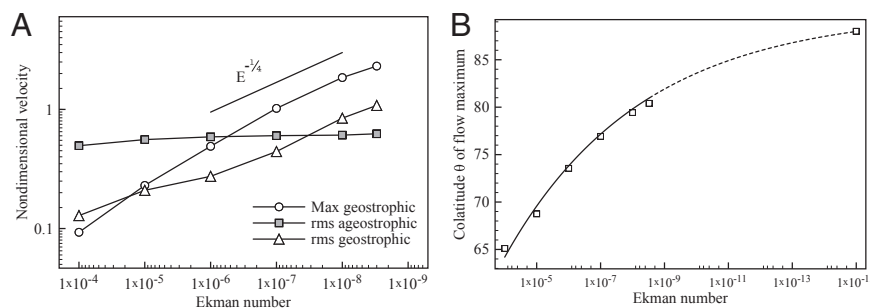


Fig. 2. (A) The rms and maximum geostrophic flow and the rms ageostrophic flow as a function of the Ekman number computed from the models. Below a threshold of approximately 6×10^{-8} , the geostrophic flow becomes dominant in rms. (B) The colatitude θ of the maximum geostrophic velocity with an extrapolation to $E = 10^{-15}$ using the empirical law $\sin\theta = 1 - 0.63E^{1/5}$.

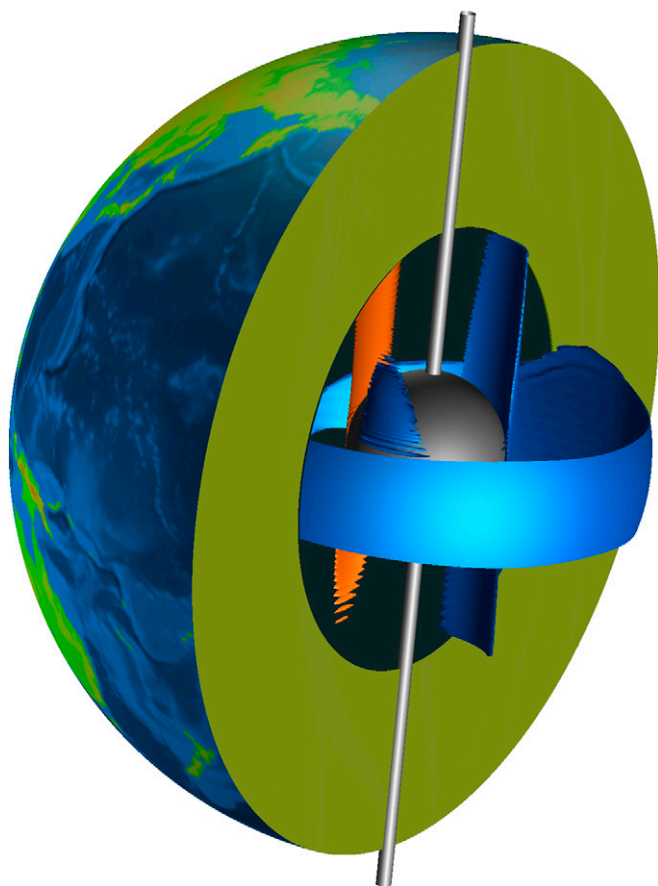


Fig. 3. Cut-away isosurface plot of u_ϕ showing the dominant westward axisymmetric equatorial jet in the model with $E=3\times 10^{-9}$; strong non-axisymmetric shear on the tangent cylinder also is visible. The contour surfaces shown are c (red, eastward) and $-c$ (blue, westward), where c is taken to be 90% of the maximum value of $|u_\phi|$. The inner core and rotation axis are shown in gray.

estimates coming from large-scale core flow inversions (24); such flows may have a significant zonal component.

Although the westward flow is of broad structure (Figs. 3 and 4), it rises to a peak close to $s=1$, creating an equatorial jet (25). Fig. 2*B* shows the location of the maximum geostrophic flow in colatitude (derived from the fit $s=\sin\theta=1-0.63E^{1/5}$ to the data). This scaling of $E^{1/5}$ is derived using empirical means but suggests a connection to the lateral extent of the equatorial viscous boundary layer, a distance from the equator that scales identically as $O(E^{1/5})$. The scaling of $E^{1/4}$, although occurring in other quantities in the model, does not fit the data well. Extrapolation to $E=10^{-15}$ shows that in the Earth-like regime, the maximum geostrophic flow would lie less than 5° from the equator. Analysis of secular variation (3) shows there is rapid change within a narrow equatorial belt (latitude -5° to $+10^\circ$), suggesting that these changes may be caused by instabilities on an equatorial jet. Furthermore, because the geostrophic flow is axisymmetric, this model predicts that the same westward jet, responsible for the westward drift in Atlantic regions, must be present in Pacific regions where secular variation is low (26). Inverse studies that determine the magnetic field strength inside the core from the motion of torsional waves show there is a local minimum in its cylindrical radial component in the outermost FOC (27). Because magnetic fields in general quench shearing motions, such a minimum is consistent with the existence of a strong equatorial jet.

We perturb the poloidal magnetic field structure to reverse its (dominant) contribution to the EM torque in region I by changing the sign of its degree 3 and 4 components (28). Our model shows that an eastward flow (of a magnitude comparable to that of the westward flow of Fig. 4*A*) was then driven in region I with an associated westward-directed torque on the inner core.

Studies of core–surface secular variation show that changes in the internal field occur on the decadal–centennial timescale of core convection (29). Assuming that the magnetic field deep inside the core changes on similar timescales, the model then predicts concomitant changes in drift direction and the rotation of the inner core relative to the mantle and, plausibly, even episodic reversals in direction. Gravitational coupling of the inner core to the mantle will dampen the rotational response of the EM torques and although poorly constrained in magnitude (30), likely has an associated inner-core deformation time of decades. We suggest that both the directions of drift and of the inner-core rotation then would be effectively enslaved to decadal–centennial secular changes in the magnetic field; in the absence of any obvious periodicity within the internal magnetic field, the inner-core rotation rate and drift velocities likely will have a non-constant and probably complex time dependence. Of particular relevance here is a recent study (31) reporting inner core rotation rates from 1961 to 2007 that are quasi-oscillatory with an ~ 20 y period, superimposed on a small constant positive (eastward) trend. Our model suggests that decadal changes in the magnetic field itself may be responsible for the fluctuations in inner-core rotation.[‡] With regard to longer timescales, our model has significant bearing on the seismically observed degree 1 structure of the inner core (8). Assuming the magnetic field had a comparable time-variation in the past as it does in the present day, the unavoidable time-dependent torques and ensuing quasi-oscillatory rotation rate likely would smear any mantle-induced texturing that otherwise would have taken place with a gravitationally locked inner core over a million-year timescale. This suggests an alternative mechanism, such as convection (33, 34), is required to explain the hemispheric structure.

It is of additional interest to identify the structure of the flow close to the tangent cylinder (the cylinder aligned with the rotation axis and tangent to the SIC), a likely location of shear layers (35). Fig. 3 shows such an asymmetric shear layer in u_ϕ , which requires high resolution to resolve. If such shear layers exist in Earth's core, instabilities could trigger torsional oscillations, which have been observed to propagate away from the tangent cylinder (27).

Finally, we remark that the magnitude of the geostrophic flow depends on E , in contrast to scaling laws derived for other quantities based on much more viscous models that are independent of viscosity (14). Ultimately, the kinetic energy of the flow must be controlled by a global energy budget and therefore independent of E as $E\rightarrow 0$, suggesting that some physics that we have neglected become important in the low- E regime. One prime candidate is inertia, whose estimated size (given by the Rossby number $R_o\approx 10^{-6}$) is comparable to $E^{1/2}\approx 10^{-7}$ in the core and thus likely is of comparable importance to viscosity. Our scalings therefore may be a valid description only for the dynamics of the modeled core in which viscosity dominates inertia, i.e., $E\gg R_o^2\approx 10^{-15}$. We speculate that the macrodynamics of u_g at core conditions then would be given by the Ekman-state description, and the dominance of inertia over viscosity at $E<10^{-15}$ would remove the singularity in u_g as $E\rightarrow 0$.

[‡]Although our model provides a consistent description of the dynamics of inner-core rotation over the 10–100-y timescale, different dynamics may be important on millennial timescales (32).

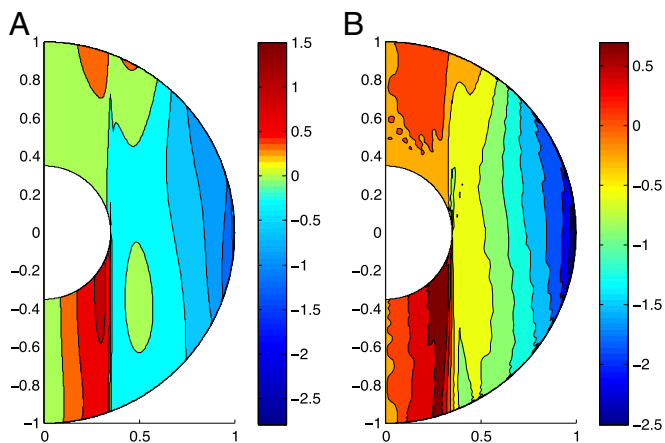


Fig. 4. Contours in a meridional plane of the axisymmetric component of the azimuthal flow u_ϕ at (A) $E = 10^{-7}$, close to the threshold at which the geostrophic flow becomes dominant; (B) $E = 3 \times 10^{-9}$ showing strong westward flow in the outermost FOC.

Methods

In a spherical shell using coordinates (r, θ, ϕ) , we evolve the coupled dimensionless Navier–Stokes and the toroidal component of the induction equation

$$R_o \frac{\partial \mathbf{u}}{\partial t} + 2\mathbf{z} \times \mathbf{u} = -\nabla \Pi + E \nabla^2 \mathbf{u} + (\nabla \times \mathbf{B}) \times \mathbf{B}, \quad [2]$$

$$\frac{\partial \mathbf{B}}{\partial t} = \nabla \times (\mathbf{u} \times \mathbf{B}) + \nabla^2 \mathbf{B} \quad [3]$$

to a steady state. The SIC (radius r_i of 0.35) is a nonslip conductor of identical electrical conductivity to the outer core; the mantle (radius 1) is modeled as a nonslip electrical insulator. In a steady state, the magnetic field satisfies $\nabla^2 \mathbf{B} = 0$ in the SIC whose solutions supply a boundary condition at the inner core boundary (ICB) for the toroidal field: evolving the magnetic field within the SIC therefore is not required. The equations have been nondimensionalized based on the core–mantle boundary radius 3,485 km (L), the magnetic diffusion timescale $T = L^2/\eta = 2 \times 10^5$ y (where η is the magnetic diffusivity), and velocity scale $U = LT^{-1} = 5 \times 10^{-7}$ ms $^{-1}$; $R_o = (\Omega T)^{-1}$ and $E = \nu(\Omega L^2)^{-1}$ then take the approximate values 10^{-9} and 10^{-15} , where Ω is the earth’s rotation rate and ν the viscosity of the fluid core. We focus only on the axial torques, associated with the manner with which the magnetic field achieves the balance required of Taylor’s constraint; because a radial buoyancy force does not contribute to these torques, we ignore any thermal or compositional driving. Following Aurnou et al. (16), the system is driven instead by prescribing the poloidal field structure: only the toroidal magnetic field and the flow are evolved; this is equivalent to the artificial insertion of a time-dependent forcing \mathbf{f} into the induction equation that renders constant the poloidal field.

The poloidal field is chosen to match the xCHAOS model (17) at epoch 2004 to degree 4, extrapolated inside the core using a smooth minimum-Ohmic-dissipation profile (36):

$$(2l+3)r^{l+1} - (2l+1)r^{l+3};$$

higher degrees of the poloidal field are zero. This particular truncation is adopted to minimize the bandwidth of the poloidal-generated Lorentz force (degree and order 8) and therefore of the flow that must be resolved, while

keeping the large-scale features of the earth’s field. Calculations using the poloidal field prescribed nonzero to degree 14 are more difficult but show the same scaling and drift direction and similar threshold Ekman number as when using degree 4.

Holding fixed the poloidal field not only allows us to impose an Earth-like structure on the system, but also suppresses the short-timescale dynamics (e.g., Alfvén waves) that prevent standard models from reaching very low viscosities. Empirical tests at $E = 10^{-6}$ show that allowing the poloidal magnetic field of degrees 5 and upward to evolve subject to the insulating boundary conditions (while keeping degrees 1–4 fixed) results in only very small differences in the eventual steady state but requires a significant drop in time step for stability. Because we seek only a steady state, stability may be improved further by taking the Rossby number to be 1 rather than $O(10^{-9})$; in so doing, we could use a time step no smaller than 0.05 (and this at the smallest E). There is no a priori guarantee that steady states exist, but if they do, it is automatic that they are independent of R_o and approach a steady Taylor state as $E \rightarrow 0$.

The poloidal and toroidal components of velocity, along with the toroidal component of magnetic field, are expanded in solid angle using spherical harmonics and in radius using Chebyshev polynomials, and the equations for their coefficients are evolved to a steady state using the second-order exponential time-differencing evolution method (37), which preserves fixed points of the equations. The nonlinear terms were evaluated using standard pseudospectral transforms; to ensure accuracy, all time-evolution matrices and spherical harmonics were computed to quadruple precision. Considerable care was taken to ensure that the calculations were converged adequately, principally in terms of the decay of their spectra. The highest resolution used was spherical harmonic degree 700, order 26 and 300 in Chebyshev degree. The code, parallelized using the Message Passing Interface (MPI), was developed especially to handle these large resolutions.

Six models were produced with decreasing values of $E = 10^{-k}$; $k = 4, 5, 6, 7, 8$; and 3×10^{-9} . The first run had zero initial conditions; each subsequent run took the final steady state of the previous as an initial condition. Because the system is nonlinear, multiple steady solutions may exist, although this process seeks only a single branch. The small generated toroidal field (taking rms values of only 2–3% of the poloidal field) is sufficient to perturb the system toward a Taylor state.

To extrapolate from our models to the earth, we note that our poloidal field is roughly three to five times weaker than expected inside the earth; this may be quantified in one of two ways: first, by the rms value of B_r on the core–mantle boundary, which for our models is 0.26 mT, three times smaller than the anticipated value of 0.69 mT from nutation studies (38); second, by the volumetric rms value of the magnetic field being 0.5 mT, two to eight times smaller than expected values of 1–4 mT (27). Because u_g depends quadratically on \mathbf{B} (principally on its poloidal component, the toroidal component being much weaker), our prescribed poloidal magnetic field will drive a geostrophic flow at least 10 times too small. Scaling up the solution using the factor of 10 discussed above, along with the dependence $E^{-1/4}$ from 10^{-7} to $E = 10^{-15}$, produces a dimensional flow of $O(10^{-4})$ m/s. Furthermore, our toroidal field is relatively small (2–3% of the poloidal field) compared with a toroidal field expected in the core of equal or larger magnitude than the poloidal field: a stronger toroidal field may drive even stronger geostrophic flows.

Further details of the model may be found in a manuscript planned for submission elsewhere.

ACKNOWLEDGMENTS. The models were run on Monte Rosa, a massively parallel Cray XE6 at the Swiss National Supercomputing Center (CSCS), Lugano, Switzerland, for which we acknowledge CSCS Grant s225. P.W.L. was supported by Natural Environment Research Council Grant NE/G014043/1. We acknowledge funding from European Research Council (ERC) Grant 247303 Magnetostrophic Flow in Experiments and the Core of the Earth (“MFECE”).

1. Jault D, Gire C, Le Mouél JL (1988) Westward drift, core motions and exchanges of angular momentum between core and mantle. *Nature* 333:353–356.
2. Jackson A (1997) Time-dependency of tangentially geostrophic core surface motions. *Phys Earth Planet Inter* 103:293–311.
3. Finlay CC, Jackson A (2003) Equatorially dominated magnetic field change at the surface of Earth’s core. *Science* 300(5628):2084–2086.
4. Dumberry M, Finlay C (2007) Eastward and westward drift of the Earth’s magnetic field for the last three millennia. *Earth Planet Sci Lett* 254:146–157.
5. Wardinski I, Korte M (2008) The evolution of the core-surface flow over the last seven thousand years. *J Geophys Res* 113:B05101.
6. Christensen U, Wicht J (2007) Numerical dynamo simulations. *Treatise on Geophysics*, ed Olson P (Elsevier, Amsterdam), Vol 8, pp 245–282.

7. Kono M, Roberts PH (2002) Recent geodynamo simulations and observations of the geomagnetic field. *Rev Geophys* 40:1–48.
8. Souriau A (2007) Deep earth structure—the earth’s cores. *Treatise on Geophysics*, eds Dziewonski AM, Romanowicz BA (Elsevier, Amsterdam), Vol 1, pp 655–693.
9. Pais A, Hulot G (2000) Length of day decade variations, torsional oscillations and inner core superrotation: Evidence from recovered core surface zonal flows. *Phys Earth Planet Inter* 118:291–316.
10. Aurnou J, Andreadis S, Zhu L, Olson P (2003) Experiments on convection in Earth’s core tangent cylinder. *Earth Planet Sci Lett* 212:119–134.
11. Kageyama A, Miyagoshi T, Sato T (2008) Formation of current coils in geodynamo simulations. *Nature* 454(7208):1106–1109.

12. Sakuraba A, Roberts PH (2009) Generation of a strong magnetic field using uniform heat flux at the surface of the core. *Nat Geosci* 2:802–805.
13. Zhan X, Zhang K, Zhu R (2011) A full-sphere convection-driven dynamo: Implications for the ancient geomagnetic field. *Phys Earth Planet Inter* 187:328–335.
14. Christensen U, Aubert J (2006) Scaling properties of convection-driven dynamos in rotating spherical shells and application to planetary magnetic fields. *Geophys J Int* 166:97–114.
15. Roberts PH, Aurnou J (2011) On the theory of core-mantle coupling. *Geophys Astrophys Fluid Dyn* 106:157–230.
16. Aurnou J, Brito D, Olson P (1998) Anomalous rotation of the inner core and the toroidal magnetic field. *J Geophys Res* 103:9721–9738.
17. Olsen N, Manda M (2008) Rapidly changing flows in the Earth's core. *Nat Geosci* 1:390–394.
18. Dumberry M, Bloxham J (2003) Torque balance, Taylor's constraint and torsional oscillations in a numerical model of the geodynamo. *Phys Earth Planet Inter* 140:29–51.
19. Fearn D (1994) Nonlinear planetary dynamos. *Lectures on Solar and Planetary Dynamos*, eds Proctor MRE, Gilbert AD (Cambridge Univ Press, Cambridge, UK), pp 219–244.
20. Jones CA (2011) Planetary magnetic fields and fluid dynamics. *Annu Rev Fluid Mech* 43:583–614.
21. Dumberry M, Mound JE (2010) Inner core-mantle gravitational locking and the super-rotation of the inner core. *Geophys J Int* 181:806–817.
22. Buffett BA, Glatzmaier GA (2000) Gravitational braking of inner-core rotation in geodynamo simulations. *Geophys Res Lett* 27:3125–3128.
23. Holme R (2007) Large-scale flow in the core. *Treatise on Geophysics*, ed Kono M (Elsevier, Amsterdam), Vol 8, pp 107–130.
24. Aubert J (2005) Steady zonal flows in spherical shell dynamos. *J Fluid Mech* 542:53–67.
25. Miyagoshi T, Kageyama A, Sato T (2010) Zonal flow formation in the Earth's core. *Nature* 463(7282):793–796.
26. Gubbins D, Gibbons SJ (2004) *Low Pacific Secular Variation* (Am Geophys Union, Washington, DC), Vol 145, pp 279–286.
27. Gillet N, Jault D, Canet E, Fournier A (2010) Fast torsional waves and strong magnetic field within the Earth's core. *Nature* 465(7294):74–77.
28. Livermore PW, Ierley G, Jackson A (2008) The structure of Taylor's constraint in three dimensions. *Proc R Soc A* 464:3149–3174.
29. Lhuillier F, Fournier A, Hulot G, Aubert J (2011) The geomagnetic secular-variation timescale in observations and numerical dynamo models. *Geophys Res Lett* 38:L09306.
30. Buffett BA (1997) Geodynamic estimates of the viscosity of the earth's inner core. *Nature* 388:571–573.
31. Tkalčić H, Young M, Bodin T, Ngo S, Sambridge M (2013) The shuffling rotation of the earth's inner core revealed by earthquake doublets. *Nat Geosci* 6:497–502.
32. Dumberry M, Bloxham J (2006) Azimuthal flows in the Earth's core and changes in length of day at millennial timescales. *Geophys J Int* 165:32–46.
33. Monnereau M, Calvet M, Margerin L, Souriau A (2010) Lopsided growth of Earth's inner core. *Science* 328(5981):1014–1017.
34. Alboussière T, Deguen R, Melzani M (2010) Melting-induced stratification above the Earth's inner core due to convective translation. *Nature* 466(7307):744–747.
35. Livermore PW, Hollerbach R (2012) Successive elimination of shear layers by a hierarchy of constraints in inviscid spherical-shell flows. *J Math Phys* 53:073104.
36. Backus G, Parker R, Constable C (1996) *Foundations of Geomagnetism* (Cambridge Univ Press, Cambridge, UK).
37. Livermore PW (2007) An implementation of the exponential time differencing scheme to the magnetohydrodynamic equations in a spherical shell. *J Comput Phys* 220:824–838.
38. Buffett BA, Mathews PA, Herring TA (2002) Modelling of nutation and precession: Effects of electromagnetic coupling. *J Geophys Res* 107:5.1–5.15.